

## Article

# Thermal Stability and the Effect of Water on Hydrogen Fluoride Generation in Lithium-Ion Battery Electrolytes Containing LiPF<sub>6</sub>

Ji Yun Han <sup>1</sup>  and Seungho Jung <sup>2,\*</sup> 

<sup>1</sup> Department of Environmental Engineering, Ajou University, 206, World cup-ro, Yeongtong-gu, Suwon-si 16499, Korea; jy0324hoho@gmail.com

<sup>2</sup> Department of Environmental & Safety Engineering, Ajou University, 206, World cup-ro, Yeongtong-gu, Suwon-si 16499, Korea

\* Correspondence: processsafety@ajou.ac.kr

**Abstract:** Lithium-ion batteries (LIBs) have been used as electrochemical energy storage devices in various fields, ranging from mobile phones to electric vehicles. LIBs are composed of a positive electrode, a negative electrode, an electrolyte, and a binder. Among them, electrolytes consist of organic solvents and lithium ion conducting salts. The electrolytes used in LIBs are mostly linear and cyclic alkyl carbonates. These electrolytes are usually based on their combinations to allow the use of Li as the anodic active component, resulting in the high power and energy density of batteries. However, these organic electrolytes have high volatility and flammability that pose a serious safety issue when exposed to extreme conditions such as elevated temperatures. At that time, these electrolytes can react with active electrode materials and release a considerable amount of heat and gas. In this study, a simultaneous thermal analysis-mass spectrometry analysis was performed on six different organic solvents to examine the effect of water on hydrogen fluoride (HF) generation temperature in the electrolyte of a LIB. The electrolytes used in the experiment were anhydrous diethyl carbonate, 1,2-dimethoxyethane, ethylene carbonate, 1,3-dioxolane, tetrahydrofurfuryl alcohol, and 2-methyl-tetrahydrofuran, each containing LiPF<sub>6</sub>. The HF formation temperature was observed and compared with that when water entered the electrolyte exposed to high-temperature conditions such as fire.

**Keywords:** lithium-ion battery electrolytes; LiPF<sub>6</sub> salt; TG/DTA-MS analysis; thermal stability; HF generation temperature



**Citation:** Han, J.Y.; Jung, S. Thermal Stability and the Effect of Water on Hydrogen Fluoride Generation in Lithium-Ion Battery Electrolytes Containing LiPF<sub>6</sub>. *Batteries* **2022**, *8*, 61. <https://doi.org/10.3390/batteries8070061>

Academic Editor: Carlos Ziebert

Received: 8 May 2022

Accepted: 14 June 2022

Published: 28 June 2022

**Publisher's Note:** MDPI stays neutral with regard to jurisdictional claims in published maps and institutional affiliations.



**Copyright:** © 2022 by the authors. Licensee MDPI, Basel, Switzerland. This article is an open access article distributed under the terms and conditions of the Creative Commons Attribution (CC BY) license (<https://creativecommons.org/licenses/by/4.0/>).

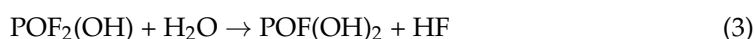
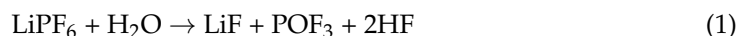
## 1. Introduction

As an important and useful electrochemical energy storage device, lithium-ion batteries (LIBs) have been developed for use in various applications ranging from mobile phones to electric vehicles [1–3]. LIBs are composed of a positive electrode, a negative electrode, an electrolyte, and a binder [4]. Among them, electrolytes consist of organic solvents and lithium ion conducting salts [5]. Many researchers have reported that electrolytes are thermally unstable at high temperatures [6,7]. Electrolytes used in LIBs are mostly linear and cyclic alkyl carbonates [8]. These electrolytes are usually based on their combinations, which allows the use of Li as the anodic active component, resulting in the high power and energy density of batteries. However, these organic electrolytes have high volatility that poses a serious safety issue when exposed to extreme conditions such as elevated temperatures [9]. In particular, the solid electrolyte interphase (SEI) formed by classical flammable carbonate liquid electrolytes can cause electrolyte decomposition, which is unstable at high temperatures [10,11]. At that time, these electrolytes can react with active electrode materials and release considerable amounts of heat and gas [12,13]. Therefore, at

high temperatures, electrolytes used in LIBs affects the thermal stability of the cell and can impact the safety of the user or the environment [14].

Lithium hexafluorophosphate ( $\text{LiPF}_6$ ) is the most widely used salt in the electrolyte of commercial LIBs [15].  $\text{LiPF}_6$  salt is easily decomposed to  $\text{LiF}$  and  $\text{PF}_5$  at room temperature, which serve as catalysts in the decomposition reaction of the solvent [16]. Fluoride ions ( $\text{F}^-$ ) generated due to the thermal decomposition of  $\text{LiPF}_6$  produce hydrogen fluoride (HF) through the reactions (1) to (5) [17]. In addition, HF is more easily generated due to hydrolysis in an unstable environment when water enters the LIB. HF is highly toxic and affects the lifespan of LIB; it promotes gas generation inside the battery cell, causing the corrosion of current collectors and the deterioration of electrode active materials [18,19]. In addition, HF is highly corrosive and toxic to human tissues, particularly the skin, eyes, bones, and tendon tissues [20].

The hydrolysis of  $\text{LiPF}_6$  is promoted by water in the electrolyte, which can generate HF by the following reaction mechanism. In the electrolyte, HF can be generated through the following reactions (1) to (3) and (4) to (5) [21].



$\text{LiPF}_6$ , which is unstable at room temperature, can generate HF through the following reactions (4) to (5) at high temperatures.



A risk assessment for the thermal decomposition of LIB has been experimentally evaluated using accelerated rate calorimetry (ARC), differential scanning calorimetry (DSC), or isothermal microcalorimetry (IMC) [22,23]. These experiments, however, pose a great burden on researchers due to the continuous escape of heat and toxic gases. In addition, experiments that analyze toxic gas species may take a long time during charging or discharging cycles of up to 20 days [24].

In this study, HF was analyzed by simultaneous thermal analysis-mass spectrometry (STA-MS) to confirm the hazards of HF generation in case of fire or high-temperature conditions in LIBs. The study aimed to compare HF generation at high temperatures between the electrolytes with and without added water.

## 2. Experimental

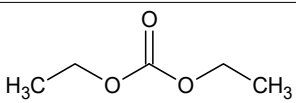
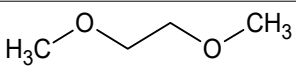
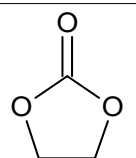
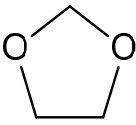
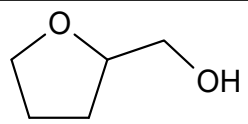
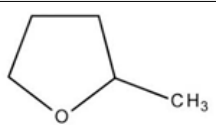
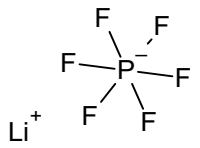
### 2.1. Preparation of Electrolyte Solutions

Organic solvents containing lithium salt are used as electrolyte solutions in LIBs because of their high operating voltage [25]. Organic solvents commonly used in electrolyte solutions are mainly mixed with a low-viscosity linear carbonate and cyclic carbonate with a high dielectric constant. In this study, the thermal stability of each solvent corresponding to a linear carbonate and cyclic carbonate was tested and confirmed. Solvents having both volatility and toxicity were selected to analyze the risk and identify the related characteristics.  $\text{LiPF}_6$  is currently the most widely used salt in commercial batteries; solvents such as diethyl carbonate (DEC) and 1,2-dimethoxyethane (DME) have a linear structure, and others, such as ethylene carbonate (EC), 1,3-dioxolane (1,3-DL), tetrahydrofurfuryl alcohol (THFA), and 2-methyl-tetrahydrofuran (2-Me-THF) have a cyclic structure. The electrolyte in which lithium salt is dissolved has high ionic conductivity and electrochemical stability but is unstable at high temperatures. Therefore, when a LIB is exposed to a high-temperature condition, there is a risk of toxic gas generation. Therefore, the purpose of this study was

to evaluate the thermal stability of electrolyte solutions of LIBs and gas generation by electrolyte solvents when exposed to an environment of elevated temperature.

In this study, six different 1 M electrolyte solutions containing  $\text{LiPF}_6$  salt (99.9% purity; Tokyo Chemical Industry, Tokyo, Japan) were prepared. Highly toxic and volatile electrolyte organic solvents were selected for use in LIBs to consider their risk evaluation [26]. The solvents used were DEC, DME, EC, 1,3-DL, THFA, and 2-Me-THF (99.9% purity; Tokyo Chemical Industry, Tokyo, Japan). Table 1 summarizes the physicochemical properties of these electrolyte materials.

**Table 1.** Physicochemical characteristics of electrolyte materials.

Chemical Name	Chemical Structure	CAS No.	Molecular Weight (g/mol)	Boiling Point (°C)	Flash Point (°C)
Diethyl carbonate (DEC)		105-58-8	118.13	126–128	33
1,2-Dimethoxyethane (DME)		110-71-4	90.12	85	−2
Ethylene carbonate (EC)		96-49-1	88.06	248	145.5
1,3-Dioxolane (1,3-DL)		646-06-0	74.08	74	−3
Tetrahydrofurfuryl alcohol (THFA)		97-99-4	102.13	178	75
2-Methyl-tetrahydro furan (2-Me-THF)		96-47-9	86.14	78–80	−10
Lithium hexafluorophosphate ( $\text{LiPF}_6$ ) <sup>*</sup>		21324-40-3	151.91	-	-

<sup>\*</sup> The onset decomposition temperature of  $\text{LiPF}_6$  is around 169 °C.

In addition, to analyze the effect of water on gas generation and resulting temperature elevation on LIB electrolytes, experiments were conducted using electrolytes with and without added water (1000 ppm). For preparing electrolytes with added water (1000 ppm), we transferred 0.01 mL of water to the Falcon conical tube using a micropipette and then added 1 M electrolyte solution containing  $\text{LiPF}_6$  up to 10 mL in the tube.

## 2.2. Measurement of Electrolyte Solutions

To determine the thermal properties of electrolyte solutions, gas generation and the resulting temperature elevation were measured using STA-MS (Netzsch's 409 PC and QMS 403C, NETZSCH (German), Selb, Germany). The samples were sealed in a hermetic  $\text{Al}_2\text{O}_3$  crucible pan in a nitrogen-filled box with flowing nitrogen gas to maintain a constant and

stable atmosphere. Each crucible was placed in the STA-MS instrument, and electrolytes were analyzed at temperatures ranging from 35 °C to 300 °C under a constant heating rate of 2 °C/min. At this time, mass change in the gas generated during thermal decomposition was simultaneously measured, and the generated gas was confirmed through mass analysis for the hydrogen cation ( $H^+$ ) ( $m/z = 1.44$ ),  $F^-$  ( $m/z = 19$ ), HF ( $m/z = 20$ ), and cyanogen fluoride (FCN) ( $m/z = 45$ ). Mass analysis was performed according to the NIST Chemistry WebBook based on the molecular weight corresponding to each peak.

Thermogravimetry/differential thermal analysis (TG/DTA) was performed for the six electrolytes with high toxicity and volatility using the STA-MS instrument to measure the decrease in thermogravimetry. Concurrently, by confirming the peaks of  $F^-$  and HF in the mass spectrum [27], HF gas generation and the temperature of the generated HF were determined.

### 3. Result and Discussion

#### 3.1. Effect of Water on Accelerating Electrolyte Decomposition

Table 1 describes the boiling point of solvents and the decomposition temperature of salt with annotation. The boiling point of most solvents is lower than the decomposition temperature of  $LiPF_6$ . Therefore, the weight loss of some solvents occurred before the decomposition of  $LiPF_6$ .

Figure 1 shows the TG/DTA curves of DEC and DME electrolyte solutions (1 M each), which are linear organic carbonate solvents, without or with added water (1000 ppm). Figure 1a,b represent the results of 1 M  $LiPF_6$ /DEC electrolyte without and with added water, respectively. Figure 1c,d represent the results of 1 M  $LiPF_6$ /DME electrolyte without and with added water, respectively. According to the results, the DTA endothermic reaction occurred at a lower temperature when water was added, indicating the accelerated thermal decomposition of each electrolyte along with loss in weight at lower temperatures. As shown in Figure 1b, the first thermal decomposition of DEC occurred at a temperature lower than 100 °C, and an endothermic reaction occurred at 130 °C when the reaction was almost completed, whereas the first endothermic reaction occurred at 130 °C for DEC without water.

The second endothermic reaction of DME also occurred at a lower temperature when water was added than when it was not.

Figure 2 shows that THFA, 2-Me-THF, and EC, which are cyclic organic solvents, have the same effect as that of linear organic solvents (DME and DEC) when water is added to each 1 M electrolyte solution. Figure 2 represents the DTA results for electrolyte solutions containing THFA, 2-Me-THF, and EC solvents with a cyclic structure. Figure 2a,b show the results of the 1 M  $LiPF_6$ /THFA electrolyte without and with added water, respectively. Figure 2c,d reveal the results of 1 M  $LiPF_6$ /2-Me-THF electrolyte without and with added water, respectively. Figure 2e,f correspond to the results of 1 M  $LiPF_6$ /EC electrolyte without and with added water, respectively. According to the results, the thermal decomposition and endothermic reaction occurred at lower temperatures, similar to the results of DEC and DME, indicating that water may act as a catalyst [28] and accelerate the decomposition reaction of an electrolyte solution at elevated temperatures.

#### 3.2. Analysis of Gases Generated from Electrolyte Decomposition

Each electrolyte solution with dissolved  $LiPF_6$  was prepared without water and with added water, which was analyzed at temperatures up to 300 °C with a constant rise of 2 °C/min. The generation of hydrogen cation ( $H^+$ ) and  $F^-$  was common in mass spectrometry results of all electrolyte solutions; however, generation of HF and FCN was different according to electrolytes and experimental conditions.

##### 3.2.1. Hydrogen Cation ( $H^+$ ) and Fluoride Ion ( $F^-$ )

Both the hydrogen cation ( $H^+$ ,  $m/z = 1.44$ ) and fluoride ions ( $F^-$ ,  $m/z = 19$ ) were generated as shown by TG/DTA-MS results of different electrolytes. Organic solvents used

for electrolyte solutions were sources of C and H, and  $\text{LiPF}_6$  salt was an  $\text{F}^-$  source. This means that the molecules that consist of  $\text{H}^+$  and  $\text{F}^-$  can be typically generated to HF.

In other words, the presence of  $\text{H}^+$  ( $m/z = 1.44$ ) and  $\text{F}^-$  ( $m/z = 19$ ) peaks in the six electrolytes containing organic solvents and  $\text{LiPF}_6$  salt indicated that a gas having  $\text{H}^+$  and  $\text{F}^-$  such as HF can be generated.

A previous study reported that HF is generated by the hydrolysis of water in LIB containing  $\text{LiPF}_6$ . However, the reaction of  $\text{H}^+$  and  $\text{F}^-$  is spontaneous [29], and therefore, HF can also be generated without adding water in electrolytes containing organic solvents and  $\text{LiPF}_6$  salt. Collectively,  $\text{H}^+$  and  $\text{F}^-$  can react to form HF spontaneously, even in the absence of a hydrolysis reaction.

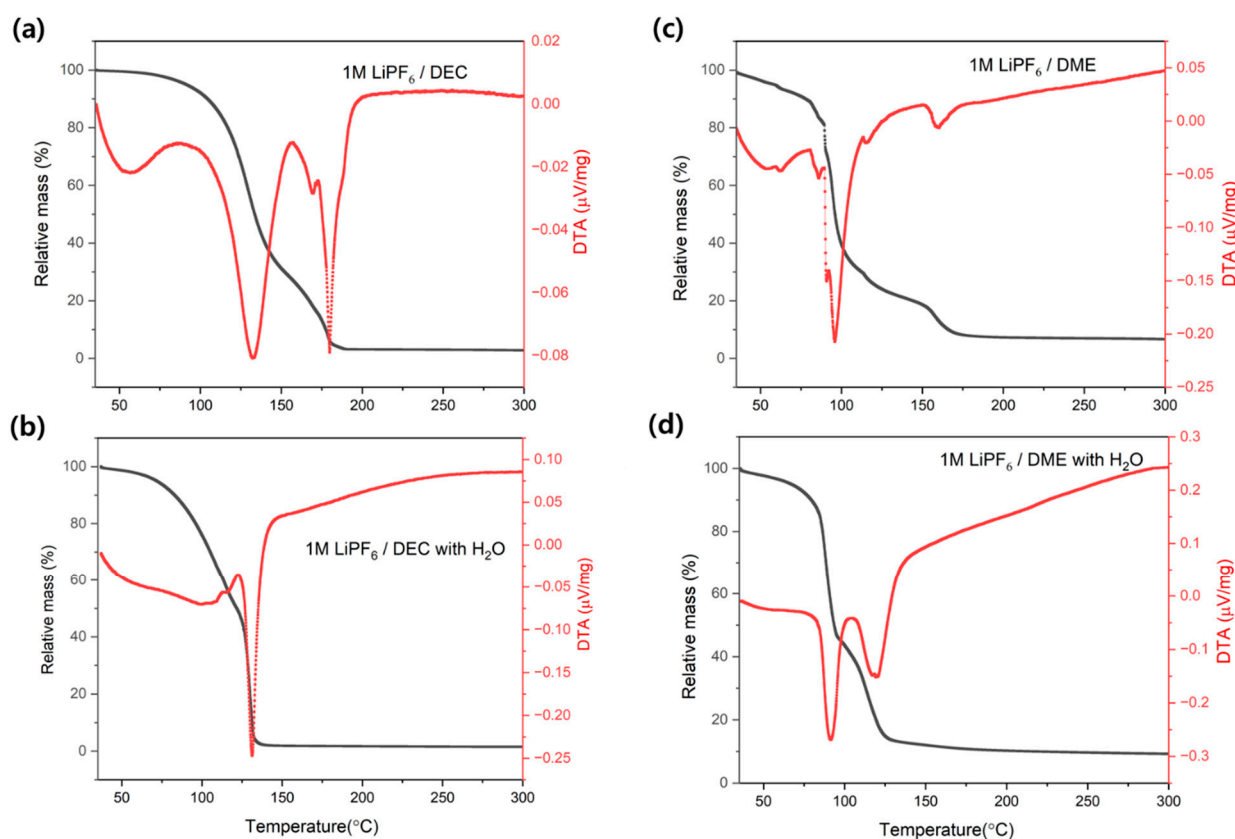


**Figure 1.** TG/DTA curves of each 1 M electrolyte solution without water (upper) and with added water (lower). (a) 1 M  $\text{LiPF}_6$ /DEC electrolyte without water, (b) 1 M  $\text{LiPF}_6$ /DEC electrolyte with added water, (c) 1 M  $\text{LiPF}_6$ /DME electrolyte without water, and (d) 1 M  $\text{LiPF}_6$ /DME electrolyte with added water.

### 3.2.2. Hydrogen Fluoride (HF)

HF was not generated in all electrolytes at elevated temperatures. HF ( $m/z = 20$ ) peak appeared in 2-Me-THF, THFA, and DME, and it was absent in DEC, EC, and 1,3-DL electrolytes when water was added to each electrolyte solution.

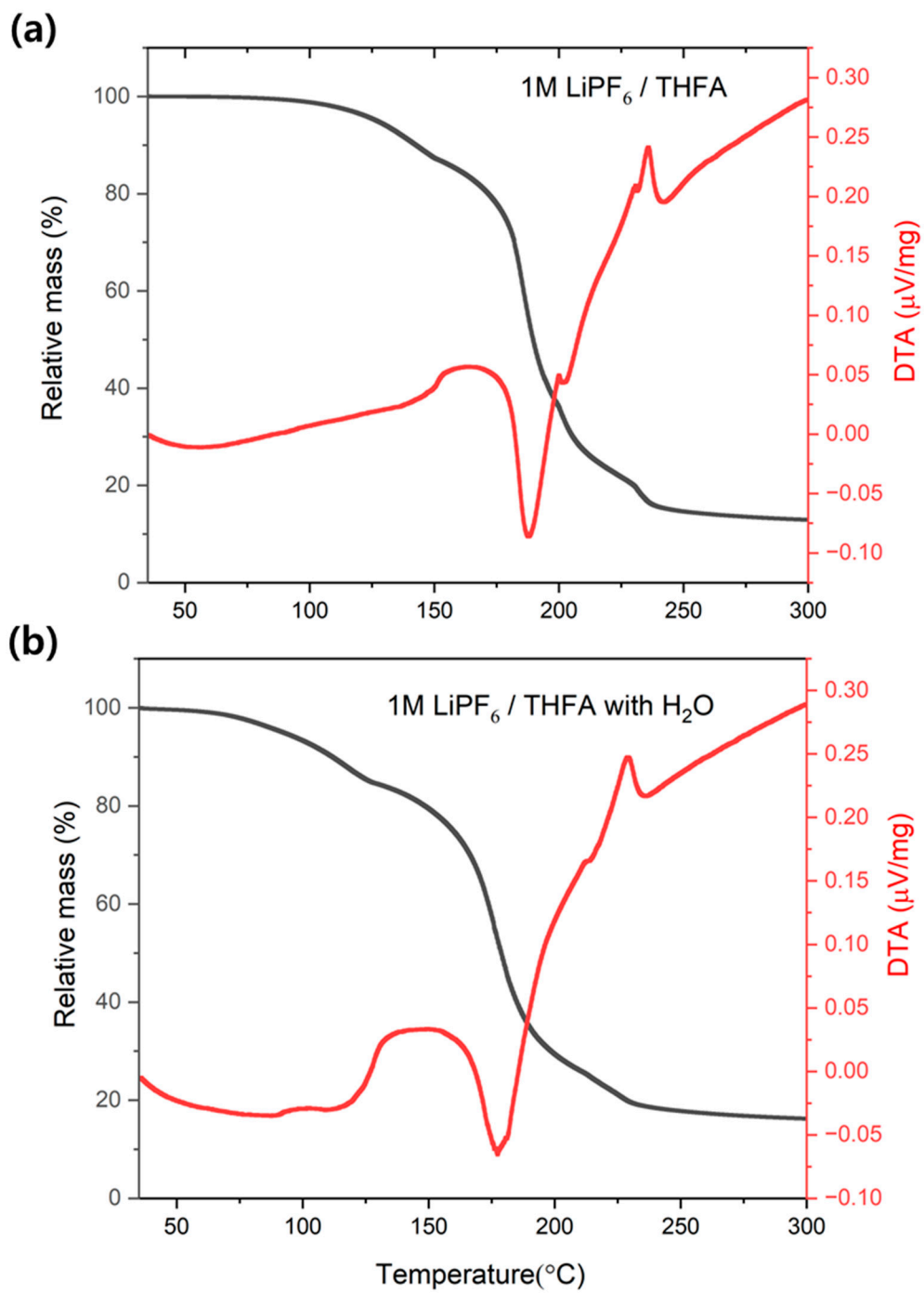


Figure 2. Cont.

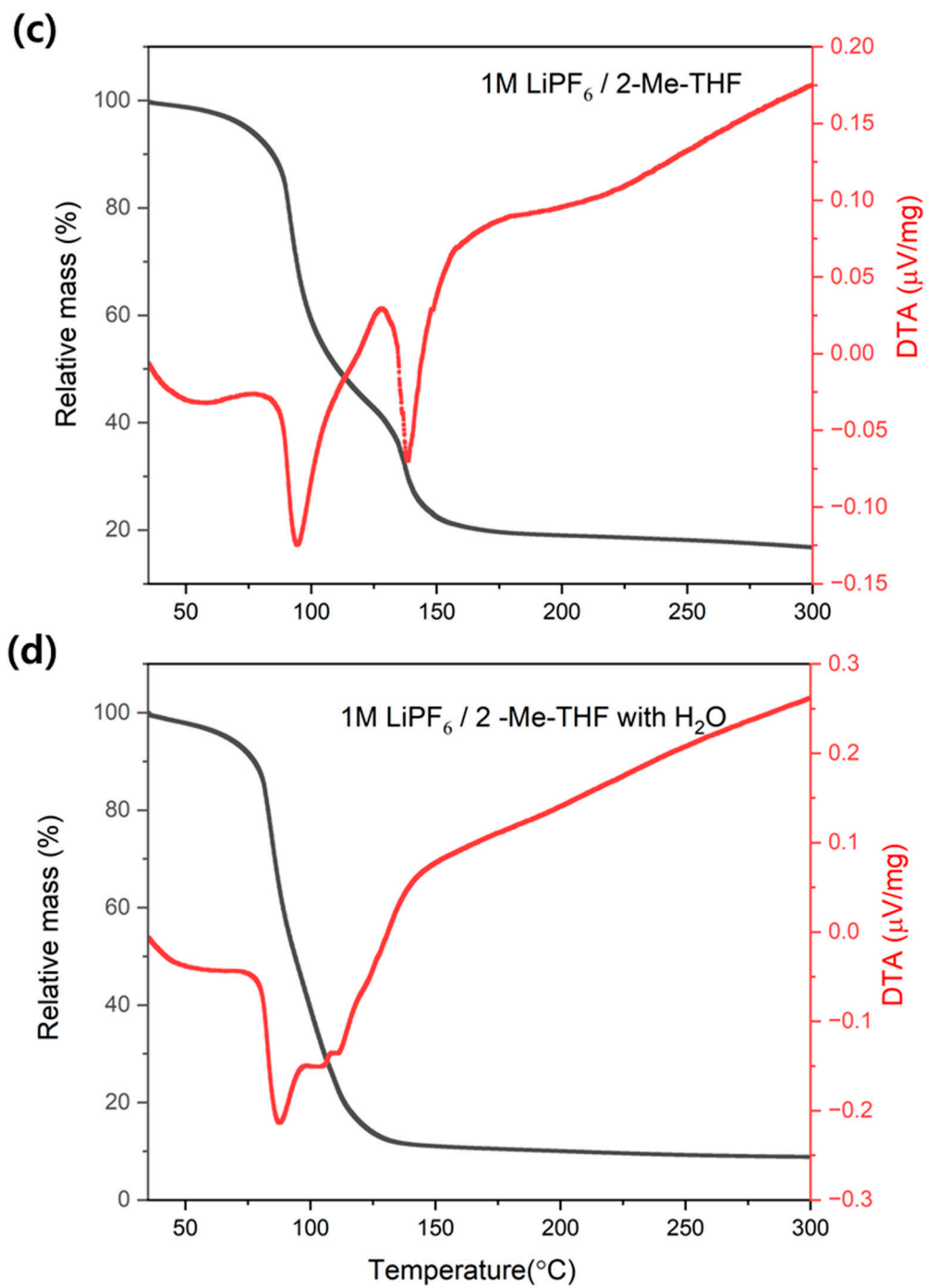
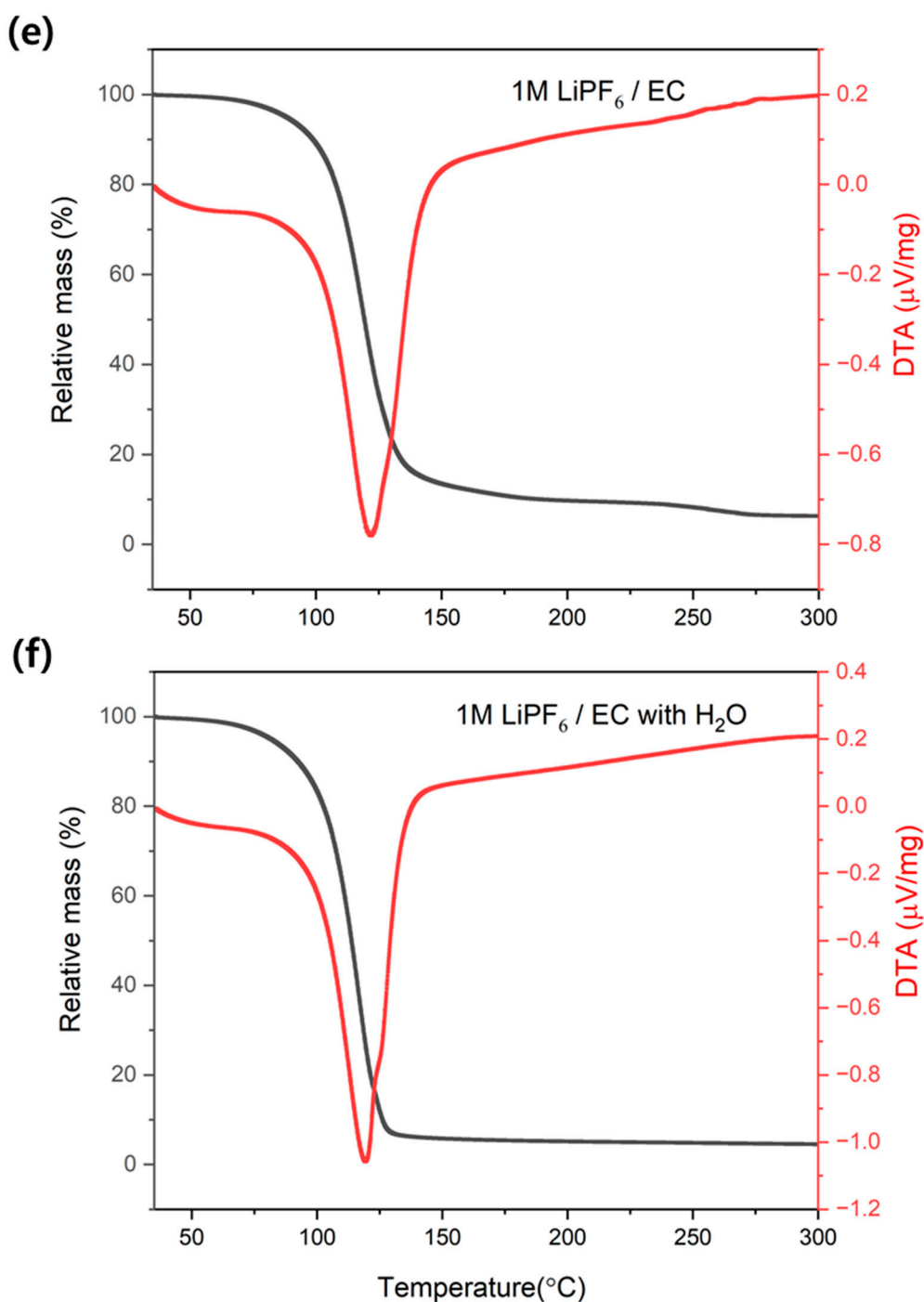


Figure 2. Cont.



**Figure 2.** TG/DTA curves of each 1 M electrolyte solution without water (upper) and with added water (lower). (a) 1 M LiPF<sub>6</sub>/THFA electrolyte without water, (b) 1 M LiPF<sub>6</sub>/THFA electrolyte with added water, (c) 1 M LiPF<sub>6</sub>/2-Me-THF electrolyte without water, (d) 1 M LiPF<sub>6</sub>/2-Me-THF electrolyte with added water, (e) 1 M LiPF<sub>6</sub>/EC electrolyte without water, and (f) 1 M LiPF<sub>6</sub>/EC electrolyte with added water.

### 3.2.3. Cyanogen Fluoride (FCN)

Figure 3 shows the results of the mass spectral peak for FCN ( $m/z = 45$ ) in 1 M LiPF<sub>6</sub>/DME and 1 M LiPF<sub>6</sub>/DEC electrolytes. FCN is a notable gas produced from decomposed electrolytes at elevated temperatures. However, the use of N<sub>2</sub> as a base gas in this experiment could be a source of FCN. Thus, FCN may not be generated in cases where N<sub>2</sub> is not used as a base gas.

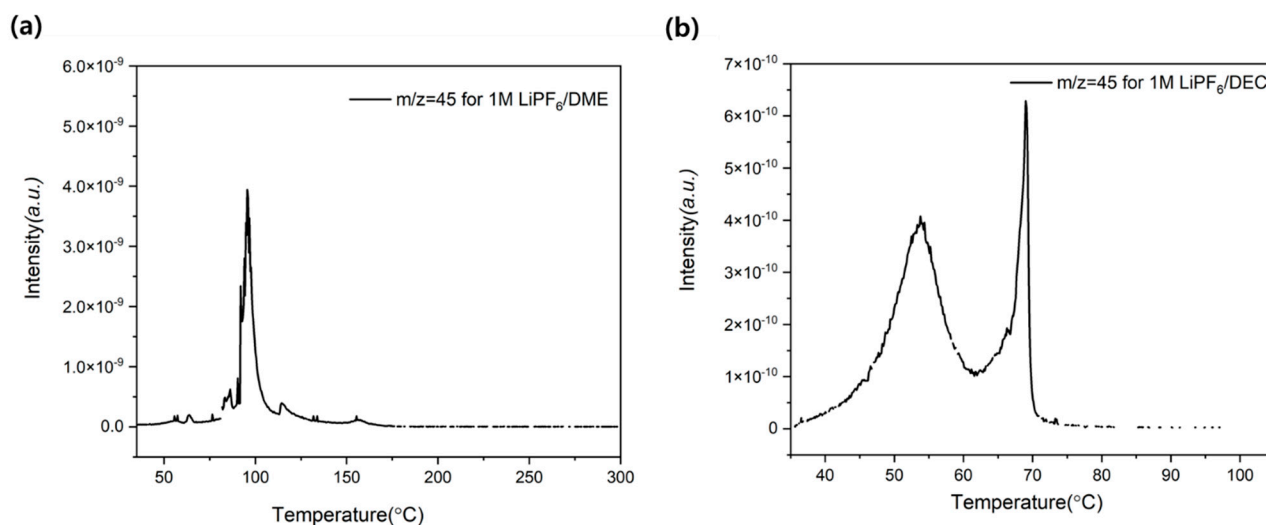


**Figure 3.** (a) Mass spectral peak of FCN ( $m/z = 45$ ) in 1 M  $\text{LiPF}_6/\text{DME}$  and (b) mass spectral peak of FCN ( $m/z = 45$ ) 1 M  $\text{LiPF}_6/\text{DEC}$  electrolyte.

Based on a previous study,  $\text{NO}_x$  gases can be generated when a LIB is exposed to high-temperature conditions. Therefore, FCN should be considered as a toxic gas generated from electrolyte decomposition [30].

FCN ( $m/z = 45$ ) peak was present in the spectra of DEC, DME, and 2-Me-THF, which has methyl groups ( $-\text{CH}_3$ ) and no double bonds in their chemical structures.

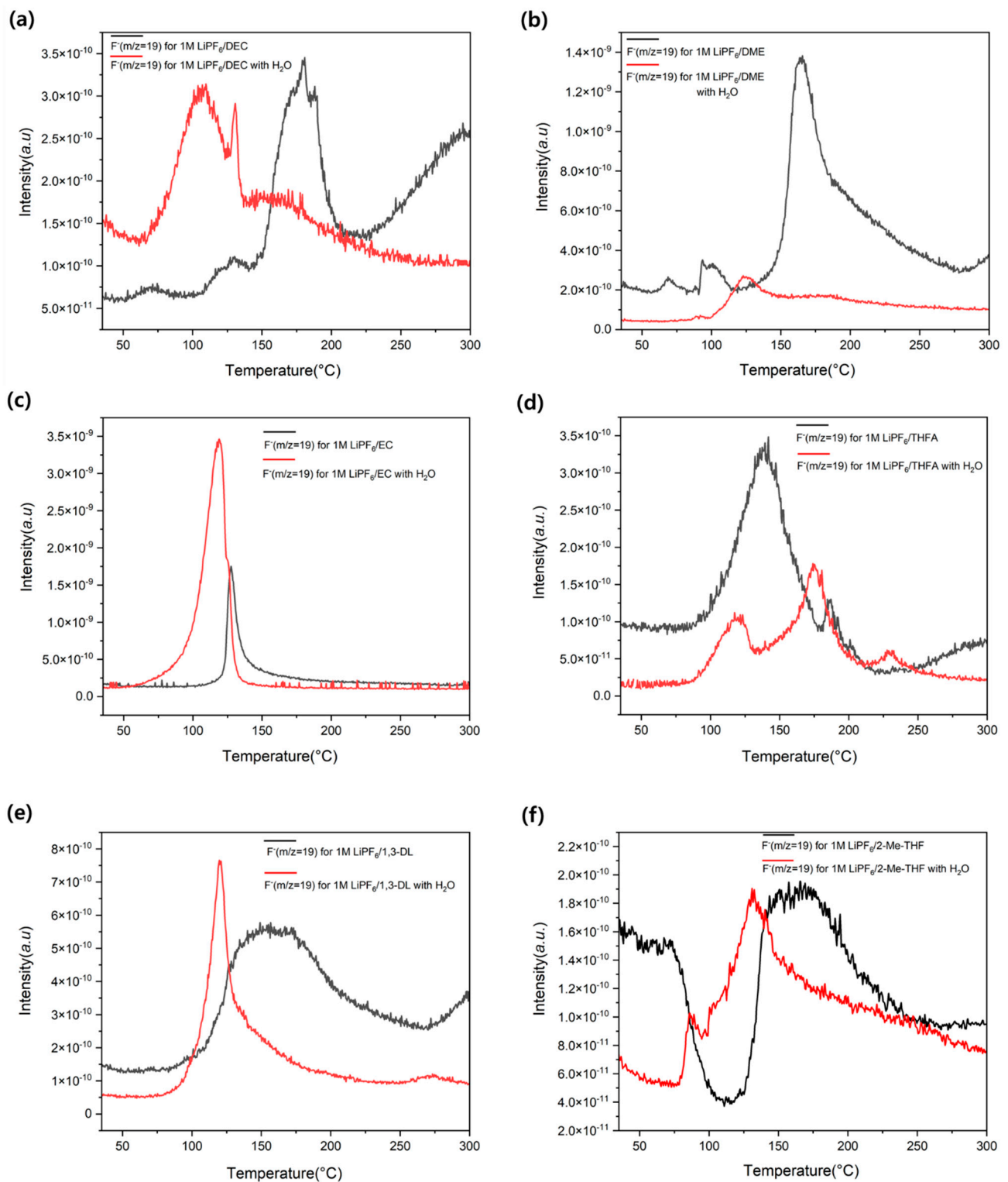
### 3.3. Effect of Water on $\text{F}^-$ Generation Temperature Shift

Figure 4 shows the results of  $\text{F}^-$  mass spectral peak in each electrolyte with and without added water.  $\text{F}^-$  generation temperature in all electrolyte solutions shifted to lower temperatures when water was added to each electrolyte.

### 3.4. Effect of Water on HF Generation Temperature Shift

#### 3.4.1. Effect of Water on HF Generation Temperature in $\text{LiPF}_6/\text{THFA}$ Electrolyte

Figures 5 and 6 show the TG/DTA-MS curves of 1 M  $\text{LiPF}_6/\text{THFA}$  electrolyte without and with added water, respectively. As shown in Figure 5, when no water was added, the first mass loss of approximately 13% was observed, and  $\text{F}^+$  ( $m/z = 19$ ) mass spectral peak intensity was high in this section. Then, the second mass loss was approximately 74%, and the HF ( $m/z = 20$ ) mass spectral peak was detected in this section. As an endothermic reaction occurred in the remaining section, the second HF peak was detected. In THFA electrolyte with added water, the  $\text{F}^+$  peak of  $\text{LiPF}_6$  was obtained between 83  $^{\circ}\text{C}$  and 186  $^{\circ}\text{C}$ , and the HF peak appeared twice during the temperature range of 160–270  $^{\circ}\text{C}$ .



**Figure 4.** Mass spectral peaks of  $F^-$  and generation temperature for each 1 M electrolyte solution containing  $LiPF_6$  with added water (red) and without water (black).  $F^-$  mass spectral peaks for (a) 1 M  $LiPF_6/DEC$ , (b) 1 M  $LiPF_6/DME$ , (c) 1 M  $LiPF_6/EC$ , (d) 1 M  $LiPF_6/THFA$ , (e) 1 M  $LiPF_6/1,3-DL$ , and (f) 1 M  $LiPF_6/2-Me-THF$ .

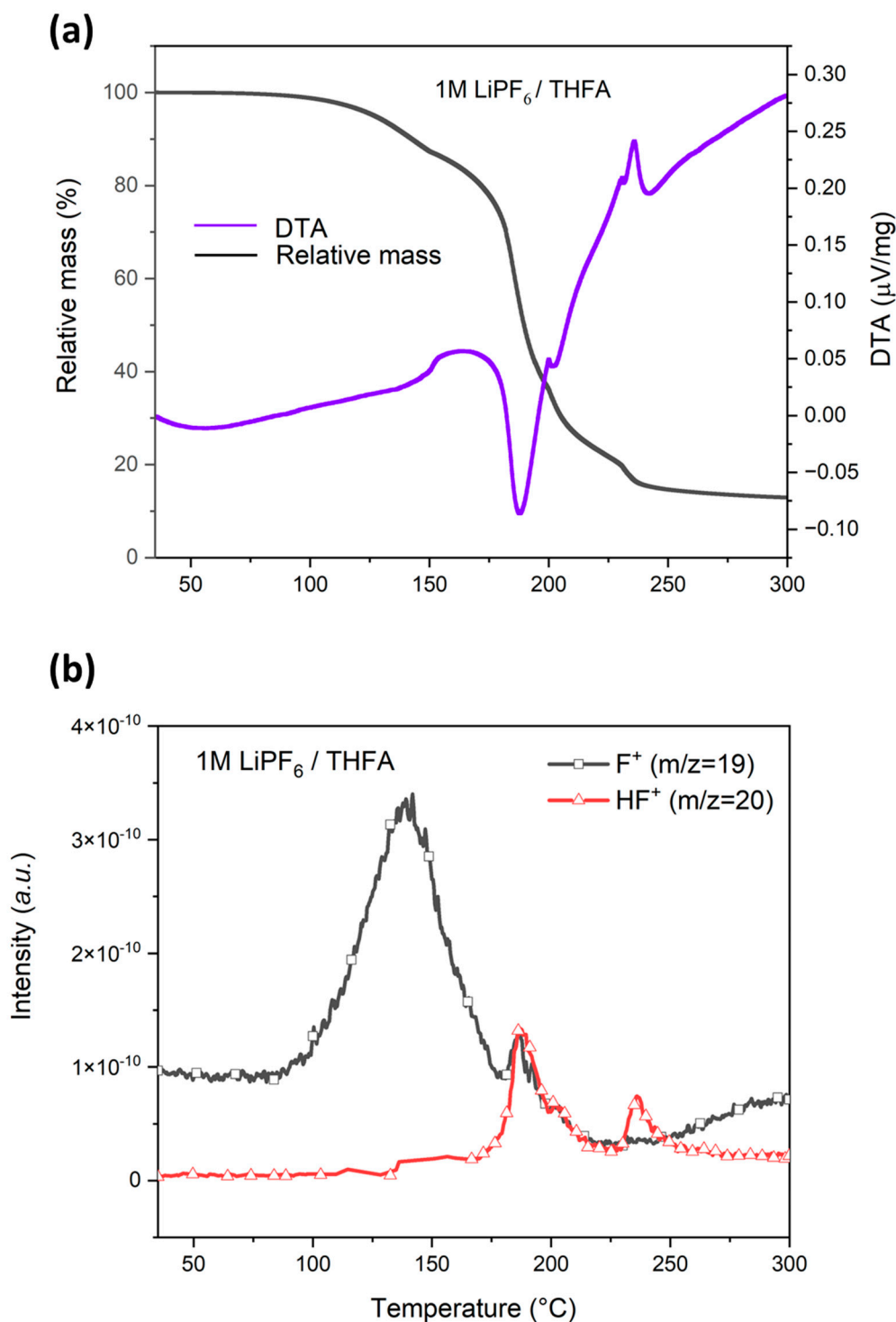


**Figure 5.** (a) TG/DTA curves of HF generation temperature in 1 M LiPF<sub>6</sub>/THFA electrolyte solution without water, and (b) the simultaneous F<sup>+</sup> and HF<sup>+</sup> identification using MS.

As shown in Figure 6, when water was added, the first mass loss of 15% and the second mass loss of 69% were observed. F<sup>+</sup> and HF peaks appeared in the first mass loss section. In the second mass loss section, both F<sup>+</sup> and HF peaks appeared, but the HF peak intensity was higher than that of the F<sup>+</sup> peak intensity. When water was added, the maximum peak intensity of F<sup>+</sup> and HF was observed in a similar temperature range with no significant difference. In THFA electrolyte with added water, F<sup>+</sup> peak was observed twice during a large temperature range of 75–220 °C, and the HF peak was observed three

times in the temperature range of 75–275 °C. The first generation of  $F^+$  and HF occurred at a lower temperature when water was added. In the solution containing water, HF was generated directly from the thermal decomposition and hydrolysis, and the peak intensity of HF ions was higher than that of  $F^+$  ions. This result shows that although pyrolysis occurs in two steps in both cases of electrolyte with and without water, there is a difference in the temperature at which HF is generated. Moreover, all HF peaks appeared during the second decomposition step; however, the result revealed the same pattern as that in the first decomposition step.

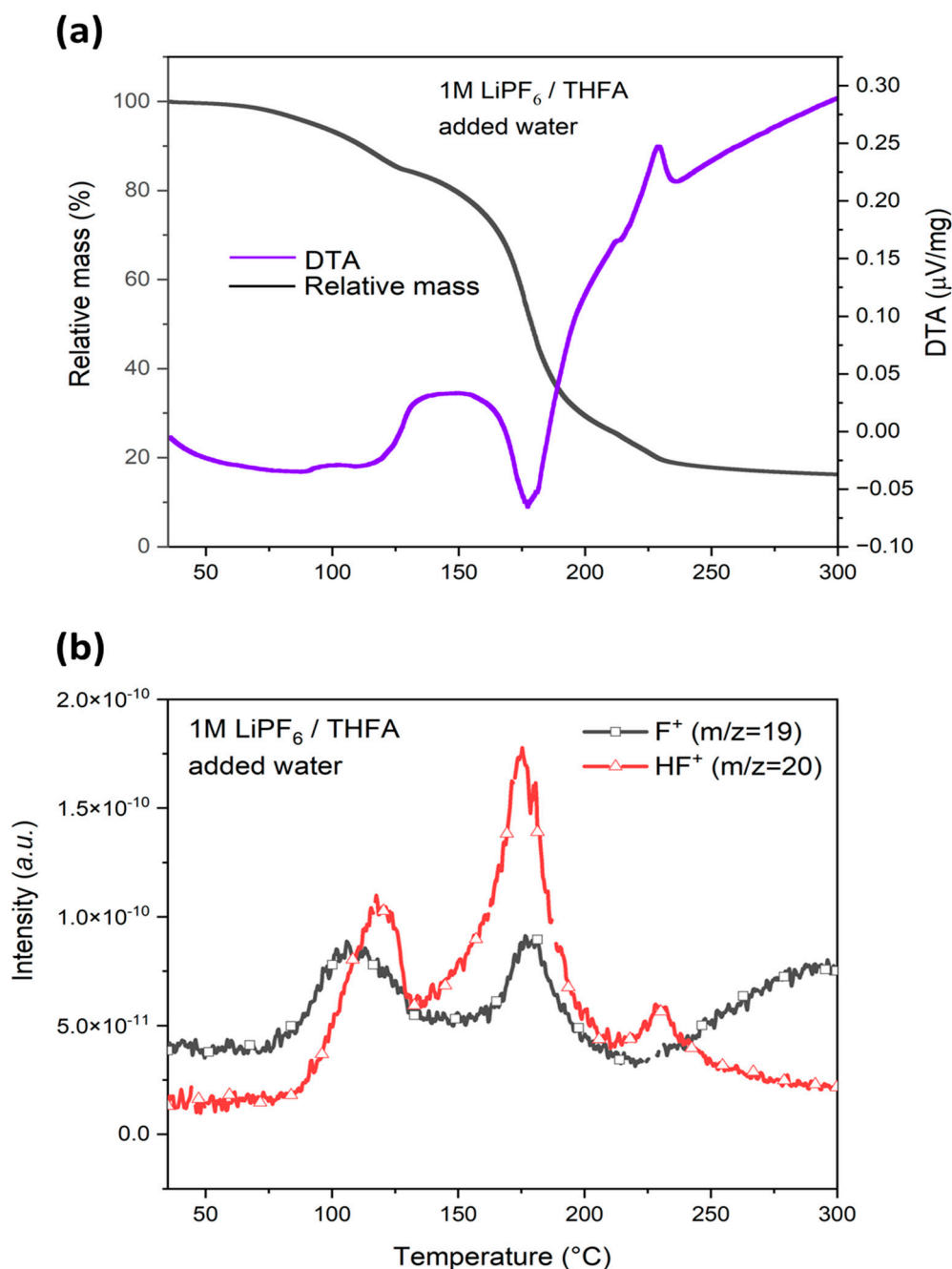


**Figure 6.** (a) TG/DTA curves of HF generation temperature in 1 M LiPF<sub>6</sub>/THFA electrolyte solution with added water, and (b) the simultaneous F<sup>+</sup> and HF<sup>+</sup> identification using MS.

#### 3.4.2. Effect of Water on HF Generation Temperature in LiPF<sub>6</sub>/2-Me-THF Electrolyte

Figures 7 and 8 show the TG/DTA-MS curves of 1 M LiPF<sub>6</sub>/2-Me-THF electrolyte without and with added water, respectively. As shown in Figure 7, in 1 M LiPF<sub>6</sub>/2-Me-THF

electrolyte without water, the first mass loss of approximately 60% occurred along with the thermal decomposition of 2-Me-THF and  $\text{LiPF}_6$ , and the  $\text{F}^+$  mass spectral peak of  $\text{LiPF}_6$  appeared. In the second mass loss section, a strong endothermic reaction occurred and a high intensity  $\text{F}^+$  peak was observed. Moreover, the  $\text{F}^+$  peak generated from  $\text{LiPF}_6$  was the highest at 138 °C in the second mass loss step. However, the HF mass spectral peak was markedly weaker than that of  $\text{F}^+$  and was not markedly differentiated. As shown in Figure 8, when water was added, two decomposition reactions occurred with 80% mass loss, and the  $\text{F}^+$  and HF peaks appeared. At this time, HF ( $m/z = 20$ ) appeared as a very strong single peak between 75 °C and 165 °C. Hence, in the 2-Me-THF electrolyte, it was confirmed that an HF peak was simultaneously generated in the temperature range of the  $\text{F}^+$  peak when water was added.

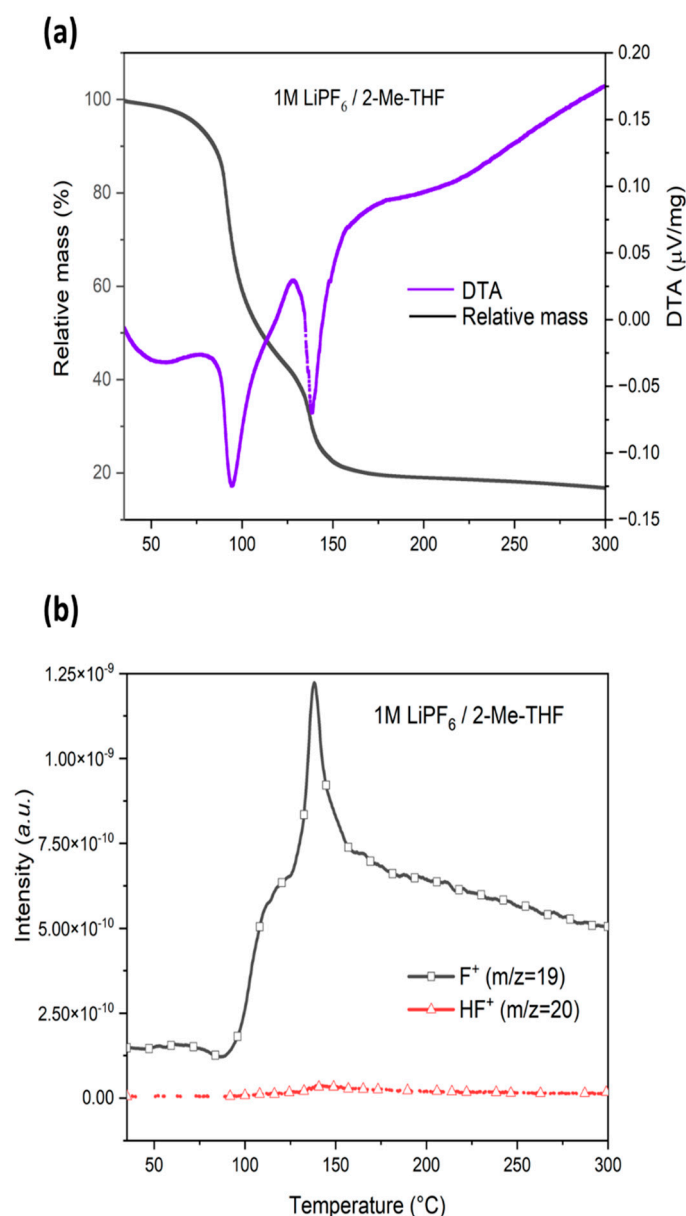


**Figure 7.** (a) TG/DTA curves of HF generation temperature in 1 M  $\text{LiPF}_6$  / 2-ME-THF electrolyte solution without water, and (b) the simultaneous  $\text{F}^+$  and  $\text{HF}^+$  identification using MS.

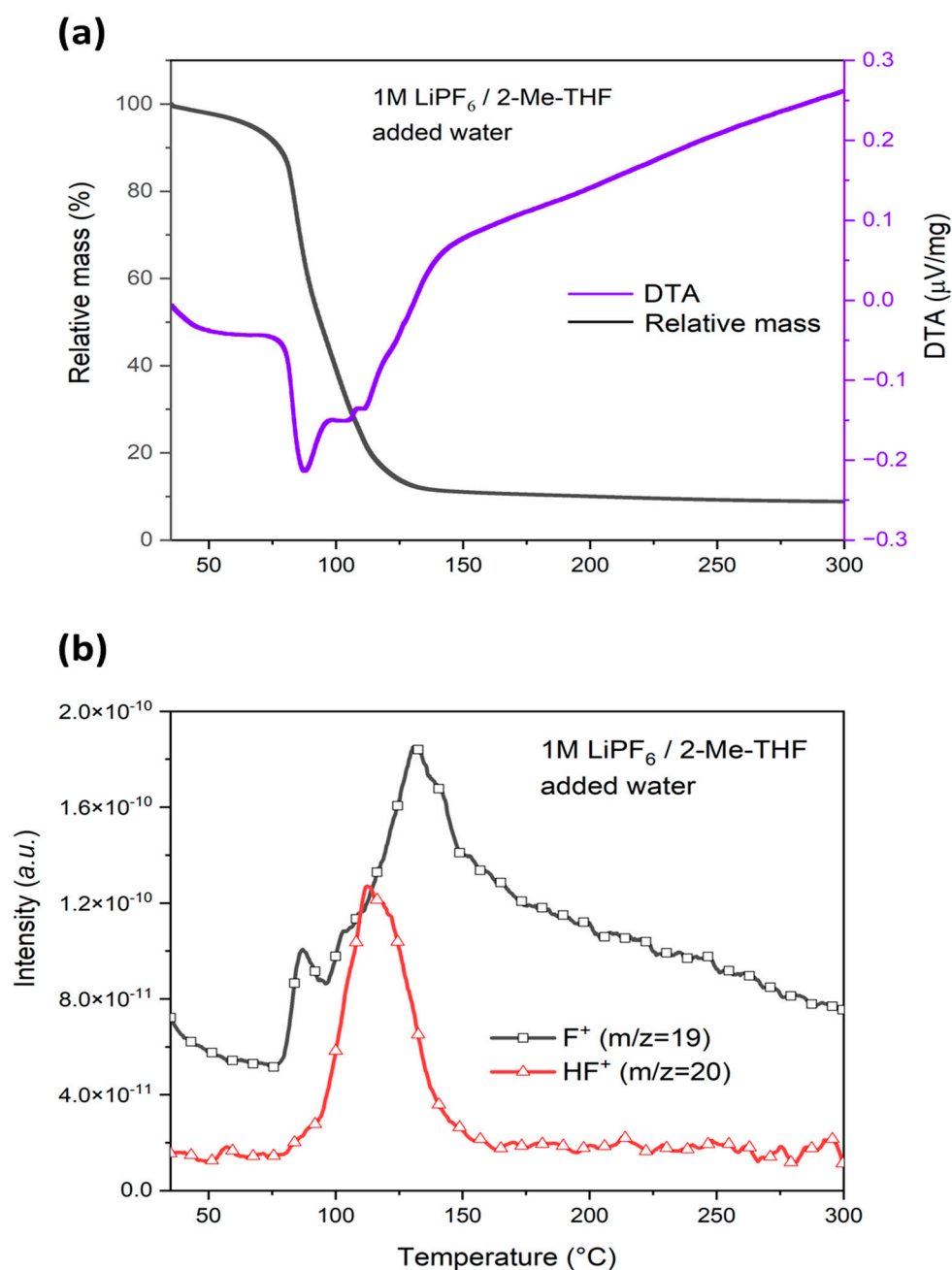


**Figure 8.** (a) TG/DTA curves of HF generation temperature in 1 M LiPF<sub>6</sub>/2-ME-THF electrolyte solution with added water, and (b) the simultaneous F<sup>+</sup> and HF<sup>+</sup> identification using MS.

### 3.4.3. Effect of Water on HF Generation Temperature in LiPF<sub>6</sub>/DME Electrolyte

Figures 9 and 10 show the TG/DTA-MS curves in 1 M LiPF<sub>6</sub>/DME electrolyte without and with added water, respectively. As shown in Figure 9, when water was not added, 83% mass loss occurred in the first section, and a very weak HF mass spectral peak at 60 °C and a relatively weak HF peak at 93 °C appeared. Since the boiling point of DME is 85 °C, it is considered that the decomposition reaction in this section is related to the boiling of the DME solvent. The second mass loss was 10% and the F<sup>+</sup> peak appeared, whereas HF was difficult to distinguish. The HF peak was observed for a short time at 93 °C, and an intense F<sup>+</sup> peak of LiPF<sub>6</sub> thermal decomposition appeared at approximately 164 °C.

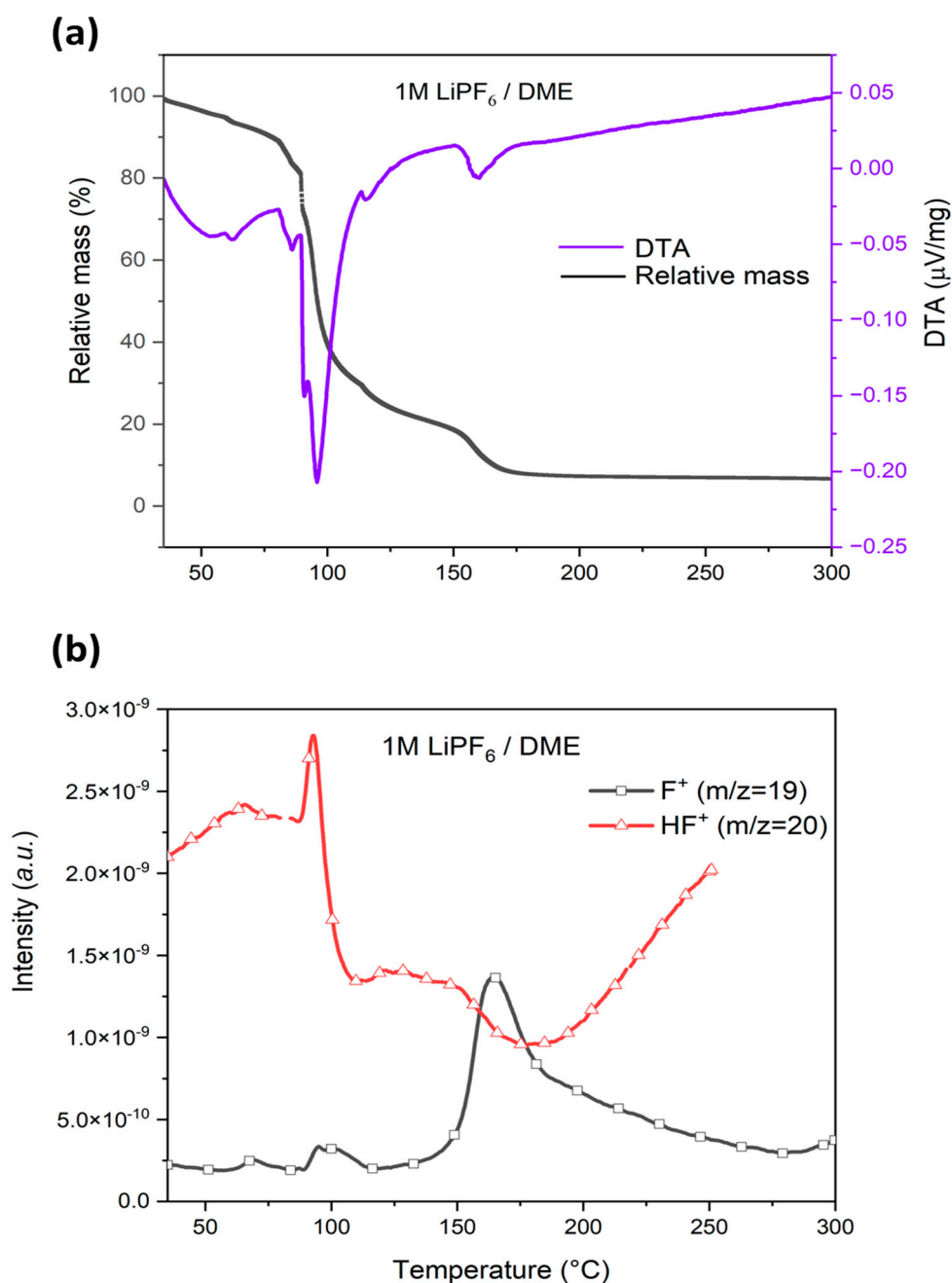


**Figure 9.** (a) TG/DTA curves of HF generation temperature in 1 M LiPF<sub>6</sub>/DME electrolyte solution without water, and (b) the simultaneous F<sup>+</sup> and HF<sup>+</sup> identification using MS.

As shown in Figure 10, the first mass loss was 54% and the second mass loss was 27% in the solution with added water, and a very strong HF peak appeared between 91 °C and 150 °C in this section. The F<sup>+</sup> spectral peak appeared in a temperature range similar to that of HF, but the HF peak occurred at a lower temperature in the electrolyte with added water than in that without water. This is because decomposition occurs more easily when water enters, and as a result, more F<sup>+</sup>, a source of HF, is generated. As shown in Figure 9a, when no water was added, the secondary endothermic reaction was the thermal decomposition of LiPF<sub>6</sub>, which occurred without any obvious difference with respect to solvent and salt. In contrast, when water was added, the temperature of the secondary endothermic reaction was lowered to 125 °C, suggesting that decomposition of LiPF<sub>6</sub> occurred immediately following the decomposition of the solvent. In the TG-DTA curves (Figure 9), when no water was added, the secondary endothermic reaction was the thermal decomposition of

LiPF<sub>6</sub>, which showed marked differences with respect to solvent and salt. However, when water was added, the temperature of the secondary endothermic reaction was lowered to 125 °C, suggesting that decomposition of LiPF<sub>6</sub> occurred immediately following the decomposition of the solvent.

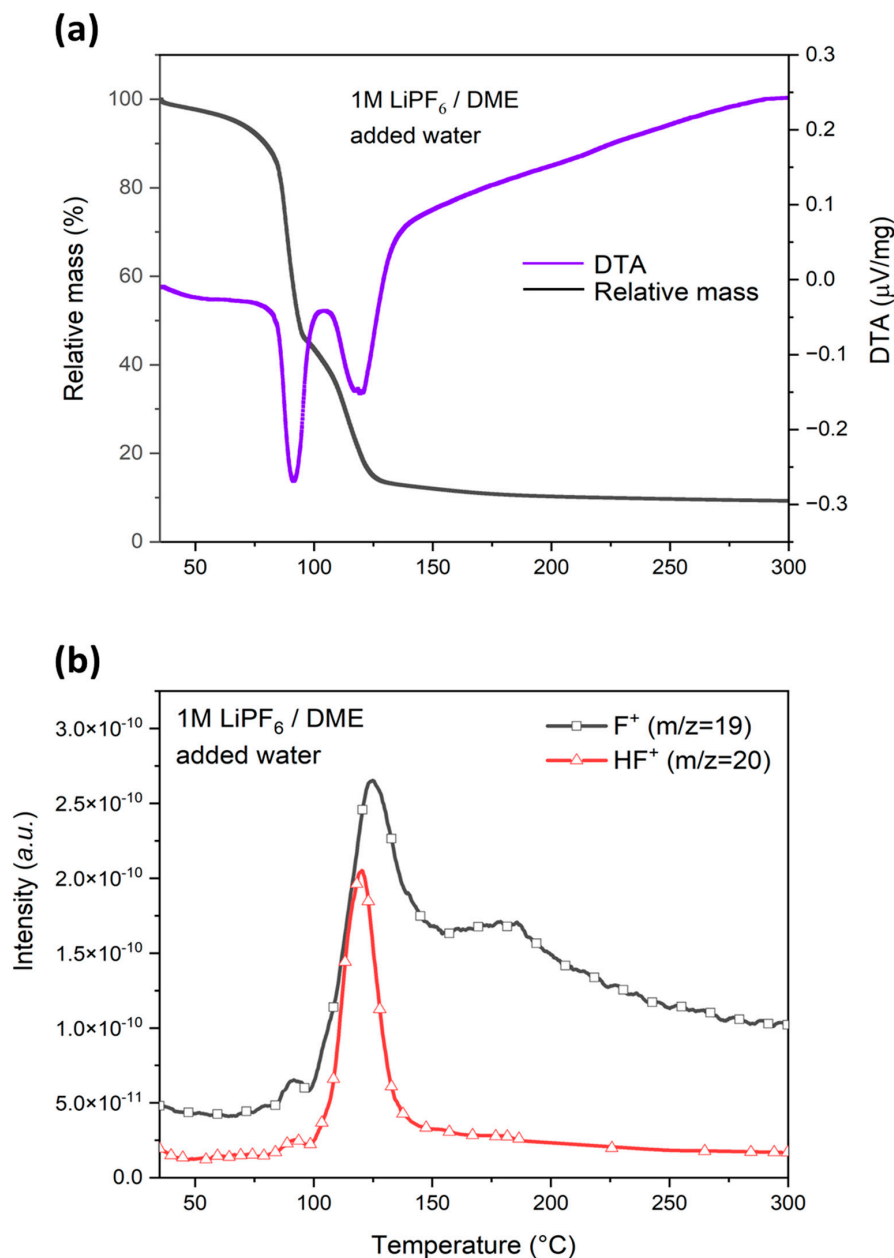


**Figure 10.** (a) TG/DTA curves of HF generation temperature in 1 M LiPF<sub>6</sub>/DME electrolyte solution with added water, and (b) the simultaneous F<sup>+</sup> and HF<sup>+</sup> identification using MS.

Table 2 summarizes the temperature and mass loss for different electrolytes without or with added water from the TG/DTA-MS analysis. According to the TG/DTA results, a two-step reaction occurred: the first was an endothermic reaction, and the second was a decomposition reaction. When water was added to THFA electrolyte, an HF peak appeared at 84 °C in the first endothermic reaction, which is lower than the boiling point (178 °C) of THFA electrolyte. In the second decomposition reaction, when water was added, an HF peak began to appear at approximately 30 °C, which is 15 °C lower than that of when water was not added. Hence, the HF generation was promoted because of the simultaneous thermal decomposition reaction due to increased temperature and hydrolysis due to added

water. In addition, the HF generation temperature in the two-step reaction in both cases of electrolyte without and with added water was lower than the boiling point of THFA electrolyte.

**Table 2.** Summary of the temperature and mass loss corresponding to TG, F<sup>+</sup> ( $m/z = 19$ ) and HF<sup>+</sup> ( $m/z = 20$ ) fragments in each electrolyte.

Solvent	Water	Step	TG <sup>a</sup> (°C)			Mass Loss (%)	F <sup>+</sup> Ion Detection Temperature <sup>b</sup>			HF Detection Temperature <sup>c</sup>		
			T <sub>i</sub>	T <sub>p</sub>	T <sub>f</sub>		T <sub>iF</sub>	T <sub>pF</sub>	T <sub>fF</sub>	T <sub>iHF</sub>	T <sub>pHF</sub>	T <sub>fHF</sub>
THFA	without water	I	75	118	150	13	83 -	139 186	179 -	-	-	-
		II	150	187	300	74	-	-	-	167 228	186 236	228 300
	added water	I	68	88	126	15	75 148	108 178	148 220	84	118	131
		II	126	177	300	69	-	-	-	131 213	175 230	213 300
2-Me-THF	without water	I	35	94	128	60	94	118	-	-	-	-
		II	128	138	300	23	118	138	300	-	140 weak	-
	added water	I	35 -	88 110	300 -	91	75 96	88 131	96 300	76	112	165
		II	128	138	300	23	118	138	300	-	140 weak	-
DME	without water	I	35	96	152	83	89	96	117	35	93	-
		II	152	161	300	10	117	164	300	-	-	>250
	added water	I	35	91	96	54	-	91 weak	-	-	91 weak	-
		II	96	119	300	37	91	124	300	91	120	150

<sup>a</sup> T<sub>i</sub> and T<sub>p</sub> are the initial and peak temperatures of TG, respectively, and T<sub>f</sub> is the final decomposition temperature.

<sup>b</sup> T<sub>iF</sub> and T<sub>pF</sub> are the initial and peak temperature of MS, respectively, and T<sub>fF</sub> is the final decomposition temperature. <sup>c</sup> T<sub>iHF</sub> and T<sub>pHF</sub> are the initial and peak temperature of MS, respectively, and T<sub>fHF</sub> is the final hydrolysis temperature.

The HF peak could not be differentiated in the 2-Me-THF electrolyte without water. However, when water was added, the HF peak began to appear at 76 °C, a temperature similar to the boiling point of the electrolyte. It could be observed that the 2-Me-THF electrolyte did not pose a great risk of HF generation when thermal decomposition occurred. However, it showed the risk of HF generation when water was added along with an increase in temperature.

In DME, unlike THFA and 2-Me-THF, when water was added, the HF peak did not appear in the first endothermic reaction, but the HF peak began to appear in the second decomposition reaction at 91 °C, 6 °C above the boiling point of DME. In addition, when no water was added, the HF peak did not appear in the first endothermic reaction in case of all electrolyte solutions. However, the HF peak began to appear at 35 °C in DME without water, and it was the lowest temperature among all temperatures at which HF peaks appeared. Therefore, the DME electrolyte showed a high risk of HF generation from the decomposition reaction, which can occur even if not exposed to high-temperature conditions.

Compared to the TG/DTA-MS results for electrolytes with added water, the MS analysis results of THFA, 2-Me-THF, and DME electrolytes showed all HF peaks between 100 °C and 150 °C. The hydrolysis reaction of LiPF<sub>6</sub> generates HF, because LiPF<sub>6</sub> dissociates into PF<sub>5</sub> in the presence of water, which acts as a strong Lewis acid, further accelerating the hydrolysis reaction. Thus, it is confirmed that the hydrolysis of LiPF<sub>6</sub> depends on the solvent. The HF mass spectral peak of THFA with added water was stronger than that of the F<sup>+</sup> mass spectral peak up to 230 °C (Figure 6), whereas the HF peak of 2-Me-THF and DME began to appear above 120 °C (Figures 8 and 10). As the temperature increased

above 120 °C, it approached 181 °C, the thermal decomposition temperature of LiPF<sub>6</sub> [31], and the peak of F<sup>+</sup>, the thermal decomposition product of LiPF<sub>6</sub>, appeared stronger. In all electrolytes except DME, the HF peak was very weak at temperatures below 100 °C, which might be related to the differences between the boiling and flash points of THFA, 2-Me-THF, and DME.

#### 4. Conclusions

HF generation from hydrolysis and the thermal decomposition of LiPF<sub>6</sub> used in LIB electrolytes and their detection temperatures were comparatively studied through TG/DTA-MS analysis. The results for electrolytes with added water and electrolytes without water were compared. The results show that LiPF<sub>6</sub> is thermally stable up to 181 °C, but F<sup>-</sup> and HF are generated at 100 °C to 150 °C in THFA, 2-Me-THF, and DME containing LiPF<sub>6</sub> when water is added to the electrolytes. LIB generates HF when exposed to high-temperature conditions. When water is added to the electrolyte, water can act as a catalyst, accelerating HF formation and lowering the HF formation temperature. This study reveals that at a temperature of 100 °C or higher, HF is generated by decomposition of LiPF<sub>6</sub> in the electrolyte due to the internal overheating of LIB, and the addition of water lowers the HF formation temperature, thereby increasing the risk of HF generation. In addition, DME among all electrolytes has a high risk of HF generation during the decomposition reaction even if it is not exposed to high-temperature conditions.

Furthermore, these results suggest what kind of organic solvents containing LiPF<sub>6</sub> salt may have a significant impact on the thermal stability of batteries and environmental safety. However, there are few studies that have investigated the influence of electrolytes on HF generation temperature during an abuse condition.

The decomposition of the most commonly used alkyl carbonate-based electrolytes start at approximately 150–200 °C. HF generated with the addition of water can cause further solvent decomposition and gas generation in electrolytes. This evolution can accompany a thermal runaway and is a safety concern. Hence, electrolytes mainly contribute to poor safety of LIB due to gas generation resulting from solvent decomposition at elevated temperatures, whether from an internal or external source.

**Author Contributions:** Conceptualization, J.Y.H.; methodology J.Y.H.; software, J.Y.H.; validation, J.Y.H. and S.J.; formal analysis, J.Y.H.; writing—original draft preparation, J.Y.H.; writing—review and editing, S.J. and J.Y.H.; visualization, J.Y.H.; supervision, S.J.; project administration, S.J. All authors have read and agreed to the published version of the manuscript.

**Funding:** Korea Ministry of Environment (MOE) (2022003620003).

**Institutional Review Board Statement:** Not applicable.

**Informed Consent Statement:** Not applicable.

**Data Availability Statement:** Not applicable.

**Acknowledgments:** This work was supported by Korea Environment Industry & Technology Institute (KEITI) through Advanced Technology Development Project for Predicting and Preventing Chemical Accidents Program, funded by Korea Ministry of Environment (MOE) (2022003620003).

**Conflicts of Interest:** The authors declare no conflict of interest.

#### References

1. Feng, X.; Ouyang, M.; Liu, X.; Lu, L.; Xia, Y.; He, X. Thermal Runaway Mechanism of Lithium Ion Battery for Electric Vehicles: A review. *Energy Storage Mater.* **2018**, *10*, 246–267. [[CrossRef](#)]
2. Cholewinski, A.; Si, P.; Uceda, M.; Pope, M.; Zhao, B. Polymer Binders: Characterization and Development toward Aqueous Electrode Fabrication for Sustainability. *Polymers* **2021**, *13*, 631. [[CrossRef](#)] [[PubMed](#)]
3. Chen, Y.; Kang, Y.; Zhao, Y.; Wang, L.; Liu, J.; Li, Y.; Liang, Z.; He, X.; Li, X.; Tavajohi, N.; et al. A Review of Lithium-ion Battery Safety Concerns: The Issues, Strategies and Testing Standards. *J. Energy Chem.* **2021**, *59*, 83–99. [[CrossRef](#)]
4. Li, Q.; Chen, J.; Fan, L.; Kong, X.; Lu, Y. Progress in Electrolytes for Rechargeable Li-based Batteries and Beyond. *Green Energy Environ.* **2016**, *1*, 18–42. [[CrossRef](#)]

5. Schultz, C.; Vedder, S.; Winter, M.; Nowak, S. Investigation of the Decomposition of Organic Solvent-based Lithium Ion Battery Electrolytes with Liquid Chromatography-mass Spectrometry. *Spectroscopyeurope* **2016**, *28*, 21–24.
6. Wang, J.; Zheng, Q.; Fang, M.; Ko, S.; Yamada, Y.; Yamada, A. Concentrated Electrolytes Widen the Operating Temperature Range of Lithium-Ion Batteries. *Adv. Sci.* **2021**, *8*, 2101646. [[CrossRef](#)]
7. Zhang, D.; Xu, X.; Ji, S.; Wang, Z.; Liu, Z.; Shen, J.; Hu, R.; Liu, J.; Zhu, M. Solvent-Free Method Prepared a Sandwich-like Nanofibrous Membrane-Reinforced Polymer Electrolyte for High-Performance All-Solid-State Lithium Batteries. *ACS Appl. Mater. Interfaces* **2020**, *12*, 21586–21595. [[CrossRef](#)]
8. Tasak, K.; Kanda, K.; Nakamura, S.; Ue, M. Decomposition of LiPF<sub>6</sub> and Stability of PF<sub>5</sub> in Li-Ion Battery Electrolytes: Density Functional Theory and Molecular Dynamics Studies. *J. Electrochem. Soc.* **2003**, *150*, A1628. [[CrossRef](#)]
9. Roth, E.P.; Orendorff, C.J. How Electrolytes Influence Battery Safety. *Electrochem. Soc. Interface* **2012**, *21*, 45. [[CrossRef](#)]
10. Wang, C.; Ouyang, L.; Fan, W.; Liu, J.; Yang, L.; Yu, L.; Zhu, M. Citraconic Anhydride as an Electrolyte Additive to Improve the High Temperature Performance of LiNi<sub>0.6</sub>Co<sub>0.2</sub>Mn<sub>0.2</sub>O<sub>2</sub>/Graphite Pouch Batteries. *J. Alloys Compd.* **2019**, *805*, 757–766. [[CrossRef](#)]
11. Wang, C.; Hu, Q.; Hao, J.; Xu, X.; Ouyang, L.; Fan, W.; Ye, J.; Liu, J.; Li, J.; Mei, A.; et al. The Electrolyte Additive Effects on Commercialized Ni-Rich LiNi<sub>x</sub>Co<sub>y</sub>Mn<sub>z</sub>O<sub>2</sub> (x + y + z = 1) Based Lithium-Ion Pouch Batteries at High Temperature. *ACS Appl. Energy Mater.* **2021**, *4*, 2292–2299. [[CrossRef](#)]
12. Zhang, Q.; Liu, K.; Ding, F.; Li, W.; Liu, X.; Zhang, J. Safety-Reinforced Succinonitrile-Based Electrolyte with Interfacial Stability for High-Performance Lithium Batteries. *ACS Appl. Mater. Interfaces* **2017**, *9*, 29820–29828. [[CrossRef](#)] [[PubMed](#)]
13. Ghiji, M.; Edmonds, S.; Moinuddin, K. A Review of Experimental and Numerical Studies of Lithium Ion Battery Fires. *Appl. Sci.* **2021**, *11*, 1247. [[CrossRef](#)]
14. Rowden, B.; Garcia-Araez, N. A Review of Gas Evolution in Lithium Ion Batteries. *Energy Rep.* **2020**, *6*, 10–18. [[CrossRef](#)]
15. Yang, H.; Zhuang, G.V.; Ross, P.V., Jr. Thermal Stability of LiPF<sub>6</sub> Salt and Li-ion Battery Electrolytes Containing LiPF<sub>6</sub>. *J. Power Sources* **2006**, *161*, 573–579. [[CrossRef](#)]
16. Lux, S.F.; Lucas, I.T.; Pollak, E.; Passerini, S.; Winter, M.; Kostecki, R. The Mechanism of HF Formation in LiPF<sub>6</sub> Based Organic Carbonate Electrolytes. *Electrochem. Commun.* **2012**, *14*, 47–50. [[CrossRef](#)]
17. Larsson, F.; Andersson, P.; Blomqvist, P.; Mellander, B.E. Toxic Fluoride Gas Emissions from Lithium-ion Battery Fires. *Sci. Rep.* **2017**, *7*, 10018. [[CrossRef](#)]
18. Chen, Y.; Liu, N.; Jie, Y.; Hu, F.; Li, Y.; Wilson, B.P.; Xi, Y.; Lai, Y.; Yang, S. Toxicity Identification and Evolution Mechanism of Thermolysis-Driven Gas Emissions from Cathodes of Spent Lithium-Ion Batteries. *ACS Sustain. Chem. Eng.* **2019**, *7*, 18228–18235. [[CrossRef](#)]
19. Pender, J.P.; Jha, G.; Youn, D.H.; Ziegler, J.M.; Andoni, I.; Choi, E.J.; Heller, A.; Dunn, B.S.; Weiss, P.S.; Penner, R.M.; et al. Electrode Degradation in Lithium-ion Batteries. *ACS Nano* **2020**, *14*, 1243–1295. [[CrossRef](#)]
20. Juba, B.W.; Mowry, C.D.; Fuentes, R.S.; Pimentel, A.S.; Román-Kustas, J.K. Lessons Learned—Fluoride Exposure and Response. *ACS Chem. Health Saf.* **2021**, *28*, 129–133. [[CrossRef](#)]
21. Solchenbach, S.; Metzger, M.; Egawa, E.; Beyer, H.; Gasteiger, H.A. Quantification of PF<sub>5</sub> and POF<sub>3</sub> from Side Reactions of LiPF<sub>6</sub> in Li-Ion Batteries. *J. Electrochem. Soc.* **2018**, *165*, A3022–A3028. [[CrossRef](#)]
22. Li, H.; Duan, Q.; Zhao, C.; Huang, Z.; Wang, Q. Experimental Investigation on the Thermal Runaway and Its Propagation in the Large Format Battery Module with Li(Ni<sub>1/3</sub>Co<sub>1/3</sub>Mn<sub>1/3</sub>)O<sub>2</sub> as Cathode. *J. Hazard. Mater.* **2019**, *375*, 241–254. [[CrossRef](#)] [[PubMed](#)]
23. Inoue, T.; Mukai, K. Roles of Positive or Negative Electrodes in the Thermal Runaway of Lithium-ion Batteries: Accelerating Rate Calorimetry Analyses with an All-inclusive Microcell. *Electrochem. Commun.* **2017**, *77*, 28–31. [[CrossRef](#)]
24. Teng, X.; Zhan, C.; Bai, Y.; Ma, L.; Liu, Q.; Wu, C.; Wu, F.; Yang, Y.; Lu, J.; Amine, K. In Situ Analysis of Gas Generation in Lithium-ion Batteries with Different Carbonate-based Electrolytes. *ACS Appl. Mater. Interfaces* **2015**, *7*, 22751–22755. [[CrossRef](#)] [[PubMed](#)]
25. Xu, K. Nonaqueous Liquid Electrolytes for Lithium-based Rechargeable Batteries. *Chem. Rev.* **2004**, *104*, 4303–4417. [[CrossRef](#)] [[PubMed](#)]
26. Lebedeva, N.P.; Boon-Brett, L. Considerations on the Chemical Toxicity of Contemporary Li-ion Battery Electrolytes and Their Components. *J. Electrochem. Soc.* **2016**, *163*, A821. [[CrossRef](#)]
27. Gaulupeau, B.; Delobel, B.; Cahen, S.; Fontana, S.; Hérold, C. Real-time Mass Spectroscopy Analysis of Li-ion Battery Electrolyte Degradation under Abusive Thermal Conditions. *J. Power Sources* **2017**, *342*, 808–815. [[CrossRef](#)]
28. Faigle, J.F.G.; Isolani, P.C.; Riveros, J.M. The Gas Phase Reaction of Fluoride(1-) and Hydroxide(1-) Ions with Alkyl Formats. *J. Am. Chem. Soc.* **1976**, *98*, 2049–2052. [[CrossRef](#)]
29. Paul, G.K.; Petre, N.; Erik, J.B. Influence of Water Contamination on the SEI Formation in Li-Ion Cells: An Operando EQCM-D Study. *ACS Appl. Mater. Interface* **2020**, *12*, 15934–15942.
30. Ribiere, P.; Grugeon, S.; Morcrette, M.; Boyanov, S.; Laruelle, S.; Marlair, G. Investigation on The Fire-induced Hazards of Li-ion Battery Cells by Fire Calorimetry. *Energy Environ. Sci.* **2012**, *5*, 5271–5280. [[CrossRef](#)]
31. Xu, M.; Xiao, A.; Li, W.; Lucht, B.L. Investigation of Lithium Tetrafluorooxalatophosphate LiPF<sub>4</sub>(C<sub>2</sub>O<sub>4</sub>) as a Lithium-Ion Battery Electrolyte for Elevated Temperature Performance. *J. Electrochem. Soc.* **2010**, *157*, A115. [[CrossRef](#)]